Quantum Information Processing (2023) 22:98
https://doi.org/10.1007/s11128-023-03839-z

Is entanglement a unique resource in quantum illumination?

MuSeong Kim[1] · Mi-Ra Hwang[1] · Eylee Jung[1] · DaeKil Park[1,2]

Received: 8 December 2021 / Accepted: 11 January 2023 / Published online: 31 January 2023

Abstract
It is well known that quantum illumination with a two-mode squeezed vacuum state as an initial entangled bipartite state achieves 6 dB quantum advantage in the error probability compared to classical coherent-state illumination. Is entanglement the only resource responsible for the quantum advantage? We explore this issue by applying the various squeezing operators to the two-mode squeezed vacuum state. Even though the operations do not decrease the bipartite entanglement, it is shown that the quantum advantage drastically decreases with increasing the squeezing parameters. Based on the fact, we conclude that entanglement is not unique resource responsible for the quantum advantage.

1 Introduction

Quantum entanglement [1–3] is known to be a physical resource in the various types of quantum information processing (QIP). It is used in many QIP such as in quantum teleportation [4, 5], superdense coding [6], quantum cloning [7], quantum cryptography [8, 9], quantum metrology [10], and quantum computers [11–13]. Quantum computing in particular attracted a lot of attention recently after IBM and Google independently created quantum computers. It is debatable whether "quantum supremacy" is achieved or not in the quantum computation.

A few years ago another type of entanglement-assisted QIP called quantum illumination [14, 15] became of interest to the research community. The purpose of this protocol is to detect low reflective objects embedded in baths of strong thermal noise. Typical quantum illumination is described in the following. The transmitter generates two entangled photons known as the signal (S) and idler (I) modes. The S mode photon is used to interrogate an unknown object hidden in the background. After receiving a

✉ DaeKil Park
dkpark@kyungnam.ac.kr

1 Department of Electronic Engineering, Kyungnam University, Changwon 631-701, Korea

2 Department of Physics, Kyungnam University, Changwon 631-701, Korea

photon from the target region, joint quantum measurement of the returned beam from target region and the retained I-mode photon is performed to decide on the absence or presence of a target. In particular, authors in Ref. [15] used the two-mode squeezed vacuum (TMSV) state as an initial entangled bipartite state between S and I modes. The most surprising result from the quantum illumination is the fact that the error probability related to detection is drastically lowered compared to classical coherent-state illumination, even if the initial entanglement between S and I modes disappears due to strong background noise. In particular, Ref. [15] obtains a quantum advantage[1] of $10\log_{10}4 \approx 6.02$ dB in terms of the error probability compared to classical illumination. An experimental realization of quantum illumination was explored in Ref. [20–24].

Quantum illumination with Gaussian states has been extended to asymmetric Gaussian hypothesis testing [25, 26]. Also, quantum illumination with non-Gaussian initial states generated by photon subtraction and addition has also been discussed [27, 28]. More recently, quantum illumination with three-mode Gaussian states was examined [29]. Another important issue in quantum illumination is the need to develop an efficient quantum receiver, where joint measurement can be performed. There have been several proposals related to quantum receivers [20, 24, 30, 31] and even their demonstrations [23, 32].

Is entanglement a unique resource responsible for quantum advantage in the quantum illumination? In this paper we explore this question by making use of squeezing operations. In Sect. 2 we briefly review Ref. [15]. In Sect. 3 we apply two single-mode squeezing operations to the TMSV state. Since the two single-mode operations are local unitary, it is obvious that the resulting state has the same entanglement with the TMSV state. Nonetheless, it is shown that the quantum advantage in the error probability reduces with increasing the squeezing parameter, and eventually the quantum disadvantage occurs when the squeezing parameter is larger than some critical value. In Sect. 4 we apply two-mode squeezing operations to the TMSV state. It is shown that the resulting state has larger entanglement than the TMSV state. In spite of larger entanglement the quantum advantage decreases with increasing the squeezing parameter. From the results of Sects. 3 and 4 we conclude that entanglement is not the only resource responsible for the quantum advantage in quantum illumination, which is summarized in Sect. 5.

2 Brief review of two-mode Gaussian quantum illumination

The authors of Ref. [15] used a TMSV state as the initial bipartite state of the S and I modes in the form:

[1] The quantum advantage was also discussed in the quantum metrology, another branch of quantum technology. In Ref. [16, 17] the quantum advantage in the measurement of frequency was discussed by making use of entangled quantum state when the environment is Markovian or non-Markovian, respectively. In Ref. [18] this quantum advantage was experimentally demonstrated by simulating the efficient quantum algorithm developed in Ref. [19]. In quantum illumination, however, the most important environment effect is a thermal noise, which is a merely classical background. In this reason we do not consider the effect of the quantum noises such as Markovian and non-Markovian noises in the illumination process.

$$|\psi\rangle_{SI} = \sum_{n=0}^{\infty} \sqrt{\frac{N_S^n}{(1+N_S)^{n+1}}} |n\rangle_S |n\rangle_I, \tag{2.1}$$

where N_S is a average photon number per signal mode. This is a zero-mean Gaussian state whose covariance matrix is

$$V_{TMSV} = \begin{pmatrix} A & 0 & C & 0 \\ 0 & A & 0 & -C \\ C & 0 & A & 0 \\ 0 & -C & 0 & A \end{pmatrix} \tag{2.2}$$

where $A = 2N_S + 1$ and $C = 2\sqrt{N_S(1+N_S)}$.

Let ρ_0 and ρ_1 be the bipartite quantum states of the returned beam from the target region and the retained I-mode photon when a target is absent and present, respectively. Both are zero-mean Gaussian states. Since, for ρ_0, the annihilation operator for the return from the target region will be $\hat{a}_R = \hat{a}_B$, where $\hat{a}_B$ is the annihilation operator for the thermal state that has an average photon number N_B, its covariance matrix can be written in the form:

$$V_0 = \begin{pmatrix} B & 0 & 0 & 0 \\ 0 & B & 0 & 0 \\ 0 & 0 & A & 0 \\ 0 & 0 & 0 & A \end{pmatrix} \tag{2.3}$$

with $B = 2N_B + 1$. For ρ_1 the return-mode's annihilation operator would be $\hat{a}_R = \sqrt{\kappa}\hat{a}_S + \sqrt{1-\kappa}\hat{a}_B$, where κ is the reflectivity from a target and $\hat{a}_B$ is the annihilation operator for a thermal state with an average photon number $N_B/(1-\kappa)$. We assume a very lossy ($\kappa \ll 1$) return from a target with a strong thermal background ($N_B \gg 1$). Then, the covariance matrix of the ρ_1 can be written in the form

$$V_1 = \begin{pmatrix} F & 0 & \sqrt{\kappa}C & 0 \\ 0 & F & 0 & -\sqrt{\kappa}C \\ \sqrt{\kappa}C & 0 & A & 0 \\ 0 & -\sqrt{\kappa}C & 0 & A \end{pmatrix} \tag{2.4}$$

where $F = 2\kappa N_S + B$.

In order to accomplish quantum illumination processing, hypothesis testing should be performed to determine whether or not a target is present. We take the null hypothesis H_0 to mean target absence and the alternative hypothesis H_1 to indicate target presence. Then, the average error probability is

$$P_E = P(H_0)P(H_1|H_0) + P(H_1)P(H_0|H_1) \tag{2.5}$$

where $P(H_0)$ and $P(H_1)$ are the prior probabilities associated with the two hypotheses. We assume $P(H_0) = P(H_1) = 1/2$ for simplicity. The two kinds of errors $P(H_1|H_0)$ and $P(H_0|H_1)$ are usually referred to as type-I (false alarm) and type-II (missed

detection) errors, respectively. Therefore, the minimization of P_E naturally requires optimal discrimination of ρ_0 and ρ_1.

If we have M identical copies of ρ_0 and ρ_1, the optimal discrimination scheme presented in Ref. [33, 34] yields the minimal error probability P_E^{min} in the form

$$P_E^{min} = \frac{1}{2}\left[1 - \frac{1}{2}||\rho_0^{\otimes M} - \rho_1^{\otimes M}||_1\right] \tag{2.6}$$

where $||A||_1 = \mathrm{Tr}\sqrt{A^\dagger A}$ denotes the trace norm of A. However, the computation of the trace norm in Eq. (2.6) becomes incredibly tedious for large M. Also, it is difficult to imagine the large M behavior of the minimal error probability from Eq. (2.6). In order to overcome these difficulties the quantum Chernoff (QC) bound was considered [35, 36]. The QC bound P_{QC} between ρ_0 and ρ_1 is defined as

$$P_{QC} = \frac{1}{2}\left(\min_{s\in[0,1]} Q_s\right)^M \tag{2.7}$$

where

$$Q_s = \mathrm{Tr}\left[\rho_0^s \rho_1^{1-s}\right]. \tag{2.8}$$

This gives a tight upper bound for P_E^{min}, i.e., $P_E^{min} \le P_{QC}$. This bound was analytically computed in several simple quantum systems [36]. However, the computation of the optimal value s_*, which minimizes Q_s, is in general highly tedious. Therefore, in Ref. [15] the quantum Bhattacharyya (QB) bound P_{QB} between ρ_0 and ρ_1 was computed, where $s = 1/2$ is chosen instead of the optimal value $s = s_*$. For this reason, P_{QB} is always larger than P_{QC} if s_* is not $1/2$. If $N_S \ll 1 \ll N_B$, the final form of the QB bound between ρ_0 and ρ_1 reduces to

$$P_{QB} \approx \frac{1}{2}\exp\left[-\frac{M}{4N_B}\frac{\kappa C^2}{A+\sqrt{A^2-1}}\right] \approx \frac{1}{2}\exp\left[-\frac{M\kappa N_S}{N_B}\right]. \tag{2.9}$$

For classical coherent-state illumination the corresponding QB bound[2] is

$$P_{QB}^{(1)} = \frac{1}{2}\exp\left[-\frac{\sqrt{1+N_B}-\sqrt{N_B}}{\sqrt{1+N_B}+\sqrt{N_B}}M\kappa N_S\right] \approx \frac{1}{2}\exp\left[-\frac{M\kappa N_S}{4N_B}\right]. \tag{2.10}$$

The difference of Eq. (2.9) from Eq. (2.10) is a missing of factor 4 in the exponent. This implies the quantum advantage of 6 dB compared to the classical coherent-state illumination.

[2] In this case $s_* = 1/2$ and hence $P_{QC} = P_{QB}$.

3 Two single-mode squeezing operations

The single-mode squeezing operation is defined as

$$\hat{S}(z) = \exp\left[\frac{1}{2}\left(z^*\hat{a}^2 - z\hat{a}^{\dagger 2}\right)\right] \tag{3.1}$$

where $z = re^{i\phi}$ and, $\hat{a}$ and $\hat{a}^\dagger$ are creation and annihilation operators, respectively. Then, two single-mode squeezing operations can be written as

$$\hat{S}(z_1, z_2) = \exp\left[\frac{1}{2}\left(z_1^*\hat{a}_1^2 - z_1\hat{a}_1^{\dagger 2}\right)\right]\exp\left[\frac{1}{2}\left(z_2^*\hat{a}_2^2 - z_2\hat{a}_2^{\dagger 2}\right)\right] = \exp\left[\frac{1}{2}\hat{r}^T\bar{H}_1\hat{r}\right] \tag{3.2}$$

where $z_i = r_i e^{i\phi_i}$, $\hat{r} = (\hat{x}_1, \hat{p}_1, \hat{x}_2, \hat{p}_2)^T$, and

$$\bar{H}_1 = \begin{pmatrix} -r_1\sin\phi_1 & r_1\cos\phi_1 \\ r_1\cos\phi_1 & r_1\sin\phi_1 \end{pmatrix} \oplus \begin{pmatrix} -r_2\sin\phi_2 & r_2\cos\phi_2 \\ r_2\cos\phi_2 & r_2\sin\phi_2 \end{pmatrix}. \tag{3.3}$$

The direct sum $\oplus$ acts on two matrices A and B such that $A \oplus B = \begin{pmatrix} A & 0 \\ 0 & B \end{pmatrix}$. Now, we choose $\phi_1 = \phi_2 = 0$ for simplicity,[3] which makes $\bar{H}_1$ to be $\bar{H}_1 = (r_1\sigma_x) \oplus (r_2\sigma_x)$, where σ_x is the x-component of the Pauli matrices.

The symplectic transform matrix M_S corresponding to $\hat{S}(r_1, r_2)$ is

$$\begin{aligned} M_S &= e^{\Omega\bar{H}_1} \\ &= \mathrm{diag}(\cosh r_1 + \sinh r_1, \cosh r_1 - \sinh r_1, \cosh r_2 + \sinh r_2, \cosh r_2 - \sinh r_2) \end{aligned} \tag{3.4}$$

where $\Omega = -i[\hat{r}, \hat{r}^T] = \begin{pmatrix} 0 & 1 \\ -1 & 0 \end{pmatrix} \oplus \begin{pmatrix} 0 & 1 \\ -1 & 0 \end{pmatrix}$. Now, we define $n_j \equiv \sinh^2 r_j$, which is the mean photon number of a squeezed vacuum state [38]. Then, M_S can be written as

$$M_S = \mathrm{diag}(\gamma_{1,+}, \gamma_{1,-}, \gamma_{2,+}, \gamma_{2,-}) \tag{3.5}$$

where $\gamma_{j,\pm} = \sqrt{n_j + 1} \pm \sqrt{n_j}$.

The operation $\hat{S}(r_1, r_2)$ on the TMSV state changes the covariance matrix to

$$V_{TSS} = M_S V_{TMSV} M_S^T = \begin{pmatrix} A\gamma_{1,+}^2 & 0 & C\gamma_{1,+}\gamma_{2,+} & 0 \\ 0 & A\gamma_{1,-}^2 & 0 & -C\gamma_{1,-}\gamma_{2,-} \\ C\gamma_{1,+}\gamma_{2,+} & 0 & A\gamma_{2,+}^2 & 0 \\ 0 & -C\gamma_{1,-}\gamma_{2,-} & 0 & A\gamma_{2,-}^2 \end{pmatrix} \tag{3.6}$$

[3] In Ref. [37] it was shown that $\phi_1 = \phi_2$ is an optimal condition under a realistic receiver.

where the subscript TSS stands for "two single-mode squeezing". It is worthwhile noting that Eq. (3.6) implies that the average photon numbers per S and I modes are

$$\tilde{N}_S = N_S + 2n_1 N_S + n_1 \qquad \tilde{N}_I = N_S + 2n_2 N_S + n_2. \tag{3.7}$$

Thus, they are different from each other if $r_1 \neq r_2$. Another point we have to note from Eq. (3.6) is the fact that the entanglement of the TSS state is exactly the same with that of the TMSV state, because the operation $\hat{S}(z_1, z_2)$ is merely a local unitary. This fact can be proved explicitly by computing the logarithmic negativities $E_{\mathcal{N}}$, which yields

$$E_{\mathcal{N}}(TMSV) = E_{\mathcal{N}}(TSS) = -2\log_2\left(\sqrt{1+N_S} - \sqrt{N_S}\right). \tag{3.8}$$

The corresponding states ρ_0 for the null hypothesis H_0 and ρ_1 for the alternative hypothesis H_1 become zero-mean Gaussian states with covariance matrices

$$V_0 = \begin{pmatrix} B & 0 & 0 & 0 \\ 0 & B & 0 & 0 \\ 0 & 0 & A\gamma_{2,+}^2 & 0 \\ 0 & 0 & 0 & A\gamma_{2,-}^2 \end{pmatrix} \tag{3.9}$$

for ρ_0 and

$$V_1 = \begin{pmatrix} F_+ & 0 & \sqrt{\kappa}C\gamma_{1,+}\gamma_{2,+} & 0 \\ 0 & F_- & 0 & -\sqrt{\kappa}C\gamma_{1,-}\gamma_{2,-} \\ \sqrt{\kappa}C\gamma_{1,+}\gamma_{2,+} & 0 & A\gamma_{2,+}^2 & 0 \\ 0 & -\sqrt{\kappa}C\gamma_{1,-}\gamma_{2,-} & 0 & A\gamma_{2,-}^2 \end{pmatrix} \tag{3.10}$$

for ρ_1, where $F_\pm = B + \kappa(A\gamma_{1,\pm}^2 - 1)$. It is straightforward to show that V_0 and V_1 reduce to the corresponding covariance matrices (2.3) and (2.4), respectively, when $\gamma_{j,\pm} = 1$. It is easy to show $\lim_{\kappa\to 0} V_1 = V_0$.

The matrix V_0 in Eq. (3.9) can be expressed as

$$V_0 = S_{V0}\begin{pmatrix} \alpha_1 \mathbb{1}_2 & 0 \\ 0 & \alpha_2 \mathbb{1}_2 \end{pmatrix} S_{V0}^T \tag{3.11}$$

where $\mathbb{1}_2$ is 2×2 identity matrix and, $\alpha_1 = B, \alpha_2 = A$, and $S_{V0} = \mathrm{diag}(1, 1, \zeta^{-1}, \zeta)$ with $\zeta = \sqrt{\gamma_{2,-}/\gamma_{2,+}}$. When deriving the symplectic eigenvalue α_2 we used $\gamma_{2,+}\gamma_{2,-} = 1$ explicitly. The matrix V_1 in Eq. (3.10) also can be expressed as

$$V_1 = S_{V1}\begin{pmatrix} \beta_1 \mathbb{1}_2 & 0 \\ 0 & \beta_2 \mathbb{1}_2 \end{pmatrix} S_{V1}^T. \tag{3.12}$$

The symplectic eigenvalues β_1 and β_2 are

$$\beta_1 = \sqrt{\frac{G + 2H + \xi}{2}} \qquad \beta_2 = \sqrt{\frac{G + 2H - \xi}{2}} \tag{3.13}$$

where $\xi = \sqrt{G^2 - 4\kappa C^2 G_+ G_-}$ and

$$\begin{aligned} G &= F_+ F_- - A^2 & H &= A^2 - \kappa C^2 \\ G_\pm &= F_\pm \gamma_{1,\mp} - A\gamma_{1,\pm} & H_\pm &= AF_\pm - \kappa C^2 \gamma_{1,\pm}^2. \end{aligned} \tag{3.14}$$

It is worthwhile noting that G, H, $G_\pm$, and $H_\pm$ are independent of $\gamma_{2,\pm}$ because they are decoupled due to the identity $\gamma_{2,+}\gamma_{2,-} = 1$. The symplectic transform S_{V1} becomes

$$S_{V1} = \begin{pmatrix} y_1 & 0 & y_5 & 0 \\ 0 & y_2 & 0 & y_6 \\ y_5' & 0 & y_3 & 0 \\ 0 & y_6' & 0 & y_4 \end{pmatrix} \tag{3.15}$$

where

$$\begin{aligned} y_1 &= \frac{\kappa C^2 G_+^2 H_+}{\sqrt{\beta_1 \xi \Delta_1}\Delta_2} \qquad y_2 = \frac{1}{2}\sqrt{\frac{\beta_1}{\xi\Delta_1}}\frac{\kappa C^2 G_+}{\Delta_2}\left[2AG_+ - \gamma_{1,+}(G - \xi)\right] \\ y_3 &= \frac{1}{2}\frac{\sqrt{\kappa} C G_+ H_+ (G + \xi)}{\sqrt{\beta_2 \xi \Delta_2}\Delta_1}\gamma_{2,+} \qquad y_4 = \frac{1}{2}\sqrt{\frac{\beta_2}{\xi\Delta_2}}\frac{\sqrt{\kappa} C G_+}{\Delta_1}\gamma_{2,-} \\ &\quad \times \left[F_+(G + \xi) - 2\kappa C^2 G_+ \gamma_{1,+}\right] \\ y_5 &= \frac{\kappa C^2 G_+^2 H_+}{\sqrt{\beta_2 \xi \Delta_2}\Delta_1} \qquad y_6 = -\frac{1}{2}\sqrt{\frac{\beta_2}{\xi\Delta_2}}\frac{\kappa C^2 G_+}{\Delta_1}\left[\gamma_{1,+}(G + \xi) - 2AG_+\right] \\ y_5' &= \frac{1}{2}\frac{\sqrt{\kappa} C G_+ H_+ (G - \xi)}{\sqrt{\beta_1 \xi \Delta_1}\Delta_2}\gamma_{2,+} \qquad y_6' = -\frac{1}{2}\sqrt{\frac{\beta_1}{\xi\Delta_1}}\frac{\sqrt{\kappa} C G_+}{\Delta_2}\gamma_{2,-} \\ &\quad \times \left[2\kappa C^2 G_+ \gamma_{1,+} - F_+(G - \xi)\right] \end{aligned} \tag{3.16}$$

with $\Delta_1 = F_+\beta_1^2 - AH_+$ and $\Delta_2 = AH_+ - F_+\beta_2^2$. When $\gamma_{1,\pm} = \gamma_{2,\pm} = 1$, it is straightforward to show that y_1, y_2, y_3, and y_4 reduce to x_+ and, y_5, y_5', $-y_6$, and $-y_6'$ to x_- where $x_\pm = \sqrt{\frac{(1+\kappa)A - \kappa + B \pm (\beta_1 + \beta_2)}{2(\beta_1 + \beta_2)}}$. This is consistent with the results of Ref. [15].

In order to compute Q_s between ρ_0 and ρ_1 given by Eq. (2.8), we define

$$\Lambda_p(x) = \frac{(x+1)^p + (x-1)^p}{(x+1)^p - (x-1)^p} \qquad G_p(x) = \frac{2^p}{(x+1)^p - (x-1)^p}. \tag{3.17}$$

Also we define

$$\Sigma_0(s) = S_{V0}\begin{pmatrix}\Lambda_s(\alpha_1)\mathbb{1}_2 & 0\\ 0 & \Lambda_s(\alpha_2)\mathbb{1}_2\end{pmatrix}S_{V0}^T$$
$$\Sigma_1(1-s) = S_{V1}\begin{pmatrix}\Lambda_{1-s}(\beta_1)\mathbb{1}_2 & 0\\ 0 & \Lambda_{1-s}(\beta_2)\mathbb{1}_2\end{pmatrix}S_{V1}^T. \tag{3.18}$$

Then, for the case of general n-mode Gaussian states ρ_0 and ρ_1 Q_s becomes [39]

$$Q_s = \bar{Q}_s \exp\Big[-(\bar{x}_0-\bar{x}_1)^T\Sigma^{-1}(s)(\bar{x}_0-\bar{x}_1)\Big] \tag{3.19}$$

where $\Sigma(s) = \Sigma_0(s) + \Sigma_1(1-s)$ and

$$\bar{Q}_s = \frac{2^n\prod_{k=1}^n G_s(\alpha_k)G_{1-s}(\beta_k)}{\sqrt{\det\Sigma(s)}}. \tag{3.20}$$

In Eq. (3.19) $\bar{x}_0$ and $\bar{x}_1$ are the mean vector of ρ_0 and ρ_1.

Since $\bar{x}_0 = \bar{x}_1 = 0$ and $n = 2$ for our case, Q_s becomes

$$Q_s = \bar{Q}_s = \frac{4G_s(\alpha_1)G_s(\alpha_2)G_{1-s}(\beta_1)G_{1-s}(\beta_2)}{\sqrt{\det\Sigma(s)}}. \tag{3.21}$$

It is straightforward to show

$$\det\Sigma(s) = \Big[x_1(s)x_3(s) - x_5^2(s)\Big]\Big[x_2(s)x_4(s) - x_6^2(s)\Big] \tag{3.22}$$

where

$$\begin{aligned}
x_1(s) &= \Lambda_s(\alpha_1) + y_1^2\Lambda_{1-s}(\beta_1) + y_5^2\Lambda_{1-s}(\beta_2)\\
x_2(s) &= \Lambda_s(\alpha_1) + y_2^2\Lambda_{1-s}(\beta_1) + y_6^2\Lambda_{1-s}(\beta_2)\\
x_3(s) &= \zeta^{-2}\Lambda_s(\alpha_2) + y_5'^2\Lambda_{1-s}(\beta_1) + y_3^2\Lambda_{1-s}(\beta_2)\\
x_4(s) &= \zeta^{2}\Lambda_s(\alpha_2) + y_6'^2\Lambda_{1-s}(\beta_1) + y_4^2\Lambda_{1-s}(\beta_2)\\
x_5(s) &= y_1y_5'\Lambda_{1-s}(\beta_1) + y_3y_5\Lambda_{1-s}(\beta_2)\\
x_6(s) &= y_2y_6'\Lambda_{1-s}(\beta_1) + y_4y_6\Lambda_{1-s}(\beta_2).
\end{aligned} \tag{3.23}$$

Therefore, the QC bound can be computed by inserting Eqs. (3.21) and (3.22) into Eq. (2.7) to obtain the optimal value s_*. In order to compute s_* we should solve

$$\left.\frac{dQ_s}{ds}\right|_{s=s_*} = 0. \tag{3.24}$$

However, it seems to be impossible to solve Eq. (3.24) analytically. Thus, in this paper, instead of finding the QC bound, we will compute the QB bound, which is defined as

$$P_{QB} = \frac{1}{2}\left(Q_{s=1/2}\right)^M. \tag{3.25}$$

Now, we assume $N_B \gg 1$ and $N_B \gg N_S$ with $\kappa \ll 1$. In this case, after a long calculation one can show

$$\begin{aligned} 4G_{1/2}(\alpha_1)G_{1/2}(\alpha_2)G_{1/2}(\beta_1)G_{1/2}(\beta_2) &\approx 16N_B(A+\sqrt{A^2-1})\left(1+\frac{K_1}{8N_B}\right) \\ \sqrt{\det\Sigma(1/2)} &\approx 16N_B(A+\sqrt{A^2-1})\left(1+\frac{K_2}{8N_B}\right) \end{aligned} \tag{3.26}$$

where

$$\begin{aligned} K_1 &= 2(2-\kappa)+\kappa A(\gamma_{1,+}^2+\gamma_{1,-}^2)-\frac{\kappa C^2}{\sqrt{A^2-1}}(\gamma_{1,+}^2+\gamma_{1,-}^2) \\ K_2 &= 2(2-\kappa)+\kappa A(\gamma_{1,+}^2+\gamma_{1,-}^2)-\frac{\kappa AC^2}{\sqrt{A^2-1}(A+\sqrt{A^2-1})}(\gamma_{1,+}^2+\gamma_{1,-}^2). \end{aligned} \tag{3.27}$$

Therefore, P_{QB} can be written approximately as

$$P_{QB} \approx \frac{1}{2}\exp\left[-\frac{M\kappa C^2}{4N_B}\frac{2n_1+1}{A+\sqrt{A^2-1}}\right]. \tag{3.28}$$

It is worthwhile noting that P_{QB} in Eq. (3.28) is independent of $\gamma_{2,\pm}$. This is due to the fact that the constraint $\gamma_{2,+}\gamma_{2,-}=1$ decouples $\gamma_{2,+}$ and $\gamma_{2,-}$ in K_1 and K_2. Thus, the squeezing operation of the second single-mode does not change the QB bound. Comparing Eq. (3.28) to a classical coherent-state illumination (2.10) with changing $N_S \to \tilde{N}_S$, one can show that a quantum advantage of our case is $10\log_{10}\Gamma_1$ (dB), where

$$\begin{aligned} \Gamma_1 &= \frac{4N_S(1+N_S)(2n_1+1)}{(N_S+2n_1N_S+n_1)\left(\sqrt{1+N_S}+\sqrt{N_S}\right)^2} \\ &= \frac{4(\tilde{N}_S-n_1)\left(\tilde{N}_S+n_1+1\right)}{\tilde{N}_S\left(\sqrt{\tilde{N}_S+n_1+1}+\sqrt{\tilde{N}_S-n_1}\right)^2}. \end{aligned} \tag{3.29}$$

When $n_1=0$ and $N_S \ll 1$, it is easy to show $\Gamma_1 \approx 4$ as expected. The r_1-dependence of Γ_1 is plotted in Fig. 1a for various N_S. This figure shows that Γ_1 decreases with increasing r_1. This can be expected because the TMSV state is nearly optimal [40–42] in the error probability for continuous-variable quantum illumination. When r_1

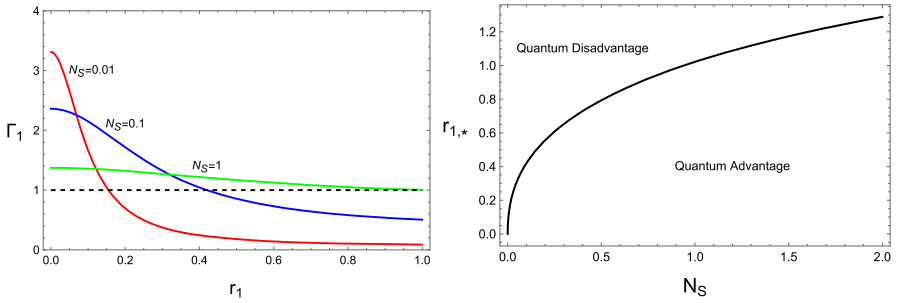

Fig. 1 (Color online) **a** The r_1-dependence of Γ_1 when $N_S = 0.01$, 0.1, and 1. This figure shows that Γ_1 decreases with increasing r_1, and eventually Γ_1 becomes less than 1 when $r_1 > r_{1,*}$. This means that the quantum disadvantage occurs in this region. This figure with Eq. (3.8) implies that entanglement is not the only resource responsible for the quantum advantage in quantum illumination. **b** The N_S-dependence of $r_{1,*}$

approaches to ∞, $\Gamma_1 - 1$ approaches to some negative value. This means that the quantum advantage disappears when $r_1 \geq r_{1,*}$. The N_S-dependence of $r_{1,*}$ is plotted in Fig. 1b. As Fig. 1b shows, $r_{1,*}$ exhibits a monotonic behavior with respect to N_S.

4 Effect of two-mode squeezing operation

In this section we examine the effects of the two-mode squeezing operation on two-mode Gaussian quantum illumination. The two-mode squeezing operation is defined as

$$\hat{S}_2(z) = \exp\left[z^* \hat{a}_1 \hat{a}_2 - z \hat{a}_1^\dagger \hat{a}_2^\dagger\right] \equiv e^{\frac{i}{2}\hat{r}^T \bar{H}_2 \hat{r}} \tag{4.1}$$

where $z = re^{i\phi}$, $\hat{r} = (\hat{x}_1, \hat{p}_1, \hat{x}_2, \hat{p}_2)^T$, and

$$\bar{H}_2 = \begin{pmatrix} 0 & r(\sigma_x \cos\phi - \sigma_z \sin\phi) \\ r(\sigma_x \cos\phi - \sigma_z \sin\phi) & 0 \end{pmatrix}. \tag{4.2}$$

Let $\phi = 0$ for simplicity. Then, the corresponding symplectic transformation matrix is

$$S_2 = e^{\Omega \bar{H}_2} = \begin{pmatrix} \mathbb{1}_2 \cosh r & \sigma_z \sinh r \\ \sigma_z \sinh r & \mathbb{1}_2 \cosh r \end{pmatrix}. \tag{4.3}$$

The $\hat{S}_2(r)$ operation on the TMSV state changes the covariance matrix to be

$$V_{TMS} = S_2 V_{TMAS} S_2^T = \begin{pmatrix} \tilde{A} & 0 & \tilde{C} & 0 \\ 0 & \tilde{A} & 0 & -\tilde{C} \\ \tilde{C} & 0 & \tilde{A} & 0 \\ 0 & -\tilde{C} & 0 & \tilde{A} \end{pmatrix} \tag{4.4}$$

where the subscript TMS stands for "two-mode squeezing" and

$$\tilde{A} = A\cosh 2r + C\sinh 2r \qquad \tilde{C} = A\sinh 2r + C\cosh 2r. \tag{4.5}$$

Eq. (4.4) implies that the average photon numbers per S and I modes are

$$\bar{N}_S = \bar{N}_I = \frac{1}{2}(\tilde{A} - 1). \tag{4.6}$$

Another point we want to note is the fact that entanglement of the TMS state can be different from that of the TMSV state, because $\hat{S}_2(z)$ is a global unitary operator. In fact, the logarithmic negativity of the TMS state is

$$E_{\mathcal{N}}(TMS) - E_{\mathcal{N}}(TMSV) = 2r\log_2 e = 2.89r \geq 0. \tag{4.7}$$

Therefore, the entanglement of TMS state is larger than that of TMSV state.

Using Eq. (4.4) one can explicitly derive the states ρ_0 and ρ_1 for the null and alternative hypotheses. Both of them are zero-mean Gaussian states whose covariance matrices are

$$V_0 = \begin{pmatrix} B & 0 & 0 & 0 \\ 0 & B & 0 & 0 \\ 0 & 0 & \tilde{A} & 0 \\ 0 & 0 & 0 & \tilde{A} \end{pmatrix} \equiv S_{V0} \begin{pmatrix} \alpha_1 \mathbb{1}_2 & 0 \\ 0 & \alpha_2 \mathbb{1}_2 \end{pmatrix} S_{V0}^T \tag{4.8}$$

for ρ_0 and

$$V_1 = \begin{pmatrix} \tilde{F} & 0 & \sqrt{\kappa}\tilde{C} & 0 \\ 0 & \tilde{F} & 0 & -\sqrt{\kappa}\tilde{C} \\ \sqrt{\kappa}\tilde{C} & 0 & \tilde{A} & 0 \\ 0 & -\sqrt{\kappa}\tilde{C} & 0 & \tilde{A} \end{pmatrix} \equiv S_{V1} \begin{pmatrix} \beta_1 \mathbb{1}_2 & 0 \\ 0 & \beta_2 \mathbb{1}_2 \end{pmatrix} S_{V1}^T \tag{4.9}$$

for ρ_1 with $\tilde{F} = \kappa\tilde{A} + B - \kappa$. One can show $\lim_{\kappa\to 0} V_1 = V_0$. The symplectic eigenvalues α_j and β_j are

$$\alpha_1 = B \quad \alpha_2 = \tilde{A} \quad \beta_k = \frac{1}{2}\left[(-1)^k(\tilde{A} - \tilde{F}) + \sqrt{(\tilde{F} + \tilde{A})^2 - 4\kappa\tilde{C}^2}\right]. \tag{4.10}$$

Also one can show that the symplectic transformation matrices are $S_{V0} = \mathbb{1}_4$ and

$$S_{V1} = \begin{pmatrix} X_+ & X_- \\ X_- & X_+ \end{pmatrix} \tag{4.11}$$

where $X_\pm = \mathrm{diag}(x_\pm, \pm x_\pm)$ with

$$x_\pm = \sqrt{\frac{\tilde{F} + \tilde{A} \pm (\beta_1 + \beta_2)}{2(\beta_1 + \beta_2)}}. \tag{4.12}$$

Using Eqs. (2.7), (3.18), (3.19), and (3.21), one can show that the QC bound is

$$P_{QC} = \frac{1}{2}\left(\min_{s\in[0,1]} \frac{4G_s(\alpha_1)G_s(\alpha_2)G_{1-s}(\beta_1)G_{1-s}(\beta_2)}{y_1(s)y_2(s) - z_3(s)^2}\right)^M \tag{4.13}$$

where

$$\begin{aligned} y_1(s) &= \Lambda_{1-s}(\beta_1)x_+^2 + \Lambda_{1-s}(\beta_2)x_-^2 + \Lambda_s(\alpha_1) \\ y_2(s) &= \Lambda_{1-s}(\beta_1)x_-^2 + \Lambda_{1-s}(\beta_2)x_+^2 + \Lambda_s(\alpha_2) \\ z_3(s) &= (\Lambda_{1-s}(\beta_1) + \Lambda_{1-s}(\beta_2))\, x_+x_-. \end{aligned} \tag{4.14}$$

Since the computation of the optimal value s_* is nontrivial, we compute the QB bound again in this case. From (4.13) the QB bound becomes

$$P_{QB} = \frac{1}{2}\left(\frac{4G_{1/2}(\alpha_1)G_{1/2}(\alpha_2)G_{1/2}(\beta_1)G_{1/2}(\beta_2)}{y_1(1/2)y_2(1/2) - z_3(1/2)^2}\right)^M. \tag{4.15}$$

If we assume $N_B \gg N_S$ and $N_B \gg 1$ with $\kappa \ll 1$, one can show

$$\begin{aligned} 4G_{1/2}(\alpha_1)G_{1/2}(\alpha_2)G_{1/2}(\beta_1)G_{1/2}(\beta_2) &\approx 16N_B\left(\tilde{A} + \sqrt{\tilde{A}^2 - 1}\right)\left(1 + \frac{J_1}{4N_B}\right) \\ y_1(1/2)y_2(1/2) - z_3(1/2)^2 &\approx 16N_B(\tilde{A} + \sqrt{\tilde{A}^2 - 1})\left(1 + \frac{J_2}{4N_B}\right) \end{aligned} \tag{4.16}$$

where

$$J_1 = (2 - \kappa + \kappa\tilde{A}) - \frac{\kappa\tilde{C}^2}{\sqrt{\tilde{A}^2 - 1}} \quad J_2 = (2 - \kappa + \kappa\tilde{A}) - \frac{\kappa\tilde{C}^2\tilde{A}}{\sqrt{\tilde{A}^2 - 1}\left(\tilde{A} + \sqrt{\tilde{A}^2 - 1}\right)}. \tag{4.17}$$

Therefore, the QB bound P_{QB} becomes approximately

$$P_{QB} \approx \frac{1}{2}\exp\left[-\frac{M}{4N_B}\frac{\kappa\tilde{C}^2}{\tilde{A} + \sqrt{\tilde{A}^2 - 1}}\right]. \tag{4.18}$$

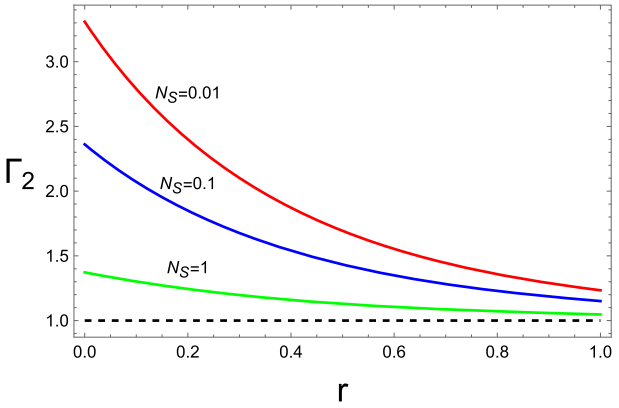

Fig. 2 (Color online) The r-dependence of Γ_2 when $N_S = 0.01$, 0.1, and 1. This figure shows that Γ_2 decreases with increasing r. This figure with Eq. (4.7) implies that entanglement is not the only resource responsible for the quantum advantage in quantum illumination

Comparing Eq. (4.18) to a classical coherent-state illumination (2.10) with changing $N_S \to \bar{N}_S$, one can show that the quantum advantage is $10\log_{10}\Gamma_2$ (dB), where

$$\Gamma_2 = \frac{\tilde{C}^2}{\bar{N}_S\left(\tilde{A} + \sqrt{\tilde{A}^2 - 1}\right)}. \tag{4.19}$$

The r-dependence of Γ_2 is plotted in Fig. 2 for various N_S. Like Fig. 1a Γ_2 decreases with increasing r. This figure shows that Γ_2 approaches to 1 in the $r \to \infty$ limit regardless of N_S. Thus, quantum disadvantage does not occur in this case.

5 Conclusion

It is well known that when $N_S \ll 1 \ll N_B$, quantum illumination with the TMSV state achieves a 6 dB gain compared to classical coherent-state illumination even though original entanglement completely disappears at the final stage due to strong background noise. It is believed that this quantum advantage is originated from the entanglement of the initial TMSV state. If this is right, it is very surprising because this fact implies that the benefits of entanglement can outlast entanglement itself. Is this entanglement a unique resource for the 6 dB gain? We try to give an answer in this paper to this question by introducing the squeezing operations.

First, we construct the TSS state by applying two single-mode squeezing operations to the TMSV state. It is obvious that the TSS state has the same entanglement with the TMSV state, because $\hat{S}(z_1, z_2)$ in Eq. (3.2) is merely a local unitary operator. Thus, if the entanglement is a unique origin of the 6 dB gain, the same gain should be achieved in quantum illumination with the TSS state. However, as Fig. 1 shows, the quantum advantage reduces with increasing the squeezing parameter r_1, and eventually it disappears at $r_1 \geq r_{1,*}$.

Second, we construct the TMS state by applying the two-mode squeezing operations to the TMSV state. It is shown that the TMS state has larger entanglement than the TMSV state. In spite of larger entanglement, Fig. 2 shows that the quantum advantage in quantum illumination with the TMS state reduces with increasing the squeezing parameter r.

In fact, reduction of the quantum advantage can be expected, because it was proved in Ref. [40–42] that the TMSV state is a nearly optimal state in the error probability provided that reflectivity is extremely small. These facts implies that the initial entanglement is not the only resource for achieving the quantum advantage. Then, it is natural to ask a question: what are other resources, which are responsible for the quantum advantage of quantum illumination? Authors in Ref. [43, 44] suggested that quantum discord is a genuine resource responsible for the quantum advantage. However, it was argued in Ref. [45] that the advantage cannot be characterized by a quantum discord sorely. Further, the counterexample was found in Ref. [37], which supports Ref. [45]. In this reason, still we do not completely understand the genuine resource in quantum illumination. We hope to visit this issue in the future.

Acknowledgements This work was supported by the National Research Foundation of Korea(NRF) grant funded by the Korea government(MSIT) (No. 2021R1A2C1094580).

Data Availibility All data generated or analysed during this study are included in this published article.

References

1. Schrödinger, E.: Die gegenwärtige Situation in der Quantenmechanik. Naturwissenschaften **23**, 807 (1935)
2. Nielsen, M.A., Chuang, I.L.: Quantum computation and quantum information. Cambridge University Press, Cambridge, England (2000)
3. Horodecki, R., Horodecki, P., Horodecki, M., Horodecki, K.: Quantum Entanglement. Rev. Mod. Phys. **81**, 865 (2009). [arXiv:quant-ph/0702225]
4. Bennett, C.H., Brassard, G., Crepeau, C., Jozsa, R., Peres, A., Wootters, W.K.: Teleporting an unknown quantum state via dual classical and Einstein-Podolsky-Rosen channles. Phys. Rev. Lett. **70**, 1895 (1993)
5. Luo, Y.H., et al.: Quantum teleportation in high dimensions. Phys. Rev. Lett. **123**, 070505 (2019). [arXiv:1906.09697 (quant-ph)]
6. Bennett, C.H., Wiesner, S.J.: Communication via one- and two-particle operators on Einstein-Podolsky-Rosen states. Phys. Rev. Lett. **69**, 2881 (1992)
7. Scarani, V., Lblisdir, S., Gisin, N., Acin, A.: Quantum cloning. Rev. Mod. Phys. **77**, 1225 (2005). [arXiv:quant-ph/0511088]
8. Ekert, A.K.: Quantum Cryptography Based on Bell's Theorem. Phys. Rev. Lett. **67**, 661 (1991)
9. Kollmitzer, C., Pivk, M.: Applied Quantum Cryptography. Springer, Heidelberg, Germany (2010)
10. Wang, K., Wang, X., Zhan, X., Bian, Z., Li, J., Sanders, B.C., Xue, P.: Entanglement-enhanced quantum metrology in a noisy environment. Phys. Rev. A **97**, 042112 (2018). [arXiv:1707.08790 (quant-ph)]
11. Ladd, T.D., Jelezko, F., Laflamme, R., Nakamura, Y., Monroe, C., O'Brien, J.L.: Quantum Computers. Nature **464**, 45 (2010). [arXiv:1009.2267 (quant-ph)]
12. Vidal, G.: Efficient classical simulation of slightly entangled quantum computations. Phys. Rev. Lett. **91**, 147902 (2003). [arXiv:1009.2267 (quant-ph)]
13. Arute, F., et al.: Quantum supremacy using a programmable superconducting processor. Nature **574**, 505 (2019). arXiv:1910.11333 (quant-ph)
14. Lloyd, S.: Enhanced sensitivity of photodetection via quantum illumination. Science **321**, 1463 (2008)

15. Tan, S.-H., Erkmen, B.I., Giovannetti, V., Guha, S., Lloyd, S., Maccone, L., Pirandola, S., Shapiro, J.H.: Quantum illumination with Gaussian states. Phys. Rev. Lett. **101**, 253601 (2008). [arXiv:0810.0534 (quant-ph)]
16. Huelga, S.F., Macchiavello, C., Pellizzari, T., Ekert, A.K., Plenio, M.B., Cirac, J.I.: Improvement of frequency standards with quantum entanglement. Phys. Rev. Lett. **79**, 3865 (1997). (**[quant-ph/9707104]**)
17. Chin, A.W., Huelga, S.F., Plenio, M.B.: Quantum metrology in Non-Markovian environments. Phys. Rev. Lett. **109**, 233601 (2012). [arXiv:1103.1219 (quant-ph)]
18. Long, X., He, W., Zhang, N., Tang, K., Lin, Z., Liu, H., Nie, X., Feng, G., Li, J., Xin, T., Ai, Q., Lu, D.: Entanglement-enhanced quantum metrology in colored noise by quantum Zeno effect. Phys. Rev. Lett. **129**, 070502 (2022). [arXiv:2208.05847 (quant-ph)]
19. Zhang, N., Tao, M., He, W., Chen, X., Kong, X., Deng, F., Lambert, N., Ai, Q.: Efficient quantum simulation of open quantum dynamics at various Hamiltonians and spectral densities. Front. Phys. **16**, 51501 (2021). [arXiv:2007.02303 (quant-ph)]
20. Guha, S., Erkmen, B.I.: Gaussian-state quantum-illumination receivers for target detection. Phys. Rev. A **80**, 052310 (2009). [arXiv:0911.0950 (quant-ph)]
21. Lopaeva, E.D., Berchera, I.R., Degiovanni, I.P., Olivares, S., Brida, G., Genovese, M.: Experimental realization of quantum illumination. Phys. Rev. Lett. **110**, 153603 (2013). [arXiv:1303.4304 (quant-ph)]
22. Barzanjeh, S., Guha, S., Weedbrook, C., Vitali, D., Shapiro, J.H., Pirandola, S.: Microwave quantum illumination. Phys. Rev. Lett. **114**, 080503 (2015). [arXiv:1503.00189 (quant-ph)]
23. Zhang, Z., Mouradian, S., Wong, F.N.C., Shapiro, J.H.: Entanglement-enhanced sensing in a lossy and noisy environment. Phys. Rev. Lett. **114**, 110506 (2015). [arXiv:1411.5969 (quant-ph)]
24. Zhuang, Q., Zhang, Z., Shapiro, J.H.: Optimum mixed-state discrimination for noisy entanglement-enhanced sensing. Phys. Rev. Lett. **118**, 040801 (2017). [arXiv:1609.01968 (quant-ph)]
25. Wilde, M.M., Tomamichel, M., Lloyd, S., Berta, M.: Gaussian hypothesis testing and quantum illumination. Phys. Rev. Lett. **119**, 120501 (2017). [arXiv:1608.0699 (quant-ph)]
26. Karsa, A., Spedalieri, G., Zhuang, Q., Pirandola, S.: Quantum illumination with a generic Gaussian source. Phys. Rev. Research **2**, 023414 (2020). [arXiv:2005.07733 (quant-ph)]
27. Zhang, S., Guo, J., Bao, W., Shi, J., Jin, C., Zou, X., Guo, G.: Quantum illumination with photon-subtracted continuous-variable entanglement. Phys. Rev. A **89**, 062309 (2014)
28. Fan, L., Zubairy, M.S.: Quantum illumination using non-Gaussian states generated by photon subtraction and photon addition. Phys. Rev. A **98**, 012319 (2018)
29. Jung, E., Park, D. K.: *Quantum illumination with three-mode Gaussian state*, arXiv:2107.05203 (quant-ph)
30. Guha, S.: *Receiver design to harness quantum illumination advantage*, in 2009 IEEE International Symposium on Information Theory, Seoul, (2009)., pp. 963-967. [arXiv:0902.2932 (quant-ph)]
31. Jo, Y., Lee, S., Ihn, Y.S., Kim, Z., Lee, S.Y.: Quantum illumination receiver using double homodyne detection. Phys. Rev. Research **3**, 013006 (2021). [arXiv:2008.11928 (quant-ph)]
32. Barzanjeh, S., Pirandola, S., Vitali, D., Fink, J.: Microwave quantum illumination using a digital receiver. Sci. Adv. **6**, eabb0451 (2020). [arXiv:1908.03058 (quant-ph)]
33. Sacchi, M.F.: Optimal discrimination of quantum operations. Phys. Rev. A **71**, 062340 (2005). [arXiv:quant-ph/0505183]
34. Sacchi, M.F.: Entanglement can enhance the distinguishability of entanglement-breaking channels. Phys. Rev. A **72**, 014305 (2005). [arXiv:quant-ph/0505174]
35. Audenaert, K.M.R., Calsamiglia, J., Muñoz-Tapia, R., Bagan, E., Masanes, L.L., Acin, A., Verstraete, F.: Discriminating states: the quantum Chernoff bound. Phys. Rev. Lett. **98**, 160501 (2007). [arXiv:quant-ph/0610027]
36. Calsamiglia, J., Muñoz-Tapia, R., Masanes, L.L., Acin, A., Bagan, E.: Quantum Chernoff bound as a measure of distinguishability between density matrices: application to qubit and Gaussian states. Phys. Rev. A **77**, 032311 (2008). [arXiv:0708.2343 (quant-ph)]
37. Jo, Y., Jeong, T., Kim, J., Kim, D. Y., Ihn, Y. S., Kim, Z., Lee, S. Y.: *Quantum illumination with asymmetrically squeezed two-mode light*, arXiv:2103.17006 (quant-ph)
38. Weedbrook, C., Pirandola, S., García-Patrón, R., Cerf, N.J., Ralph, T.C., Shapiro, J.H., Lloyd, S.: Gaussian quantum information. Rev. Mod. Phys. **84**, 621 (2012)
39. Pirandola, S., Lloyd, S.: Computable bounds for the discrimination of Gaussian states. Phys. Rev. A **78**, 012331 (2008). [arXiv:0806.1625 (quant-ph)]

40. Palma, G.D., Borregaard, J.: minimum error probability of quantum illumination. Phys. Rev. A **98**, 012101 (2018). [arXiv:1802.02158 (quant-ph)]
41. Nair, R., Gu, M.: Fundamental limits of quantum illumination. Optica **7**, 771 (2020). [arXiv:2002.12252 (quant-ph)]
42. Bradshaw, M., Conlon, L.O., Tserkis, S., Gu, M., Lam, P.K., Assad, S.M.: Optimal probes for continuous variable quantum illumination. Phys. Rev. A **103**, 062413 (2021). [arXiv:2010.09156 (quant-ph)]
43. Weedbrook, C., Pirandola, S., Thompson, J., Vedral, V., Gu, M.: How discord underlies the noise resilience of quantum illumination. New J. Phys. **18**, 043027 (2016). [arXiv:1312.3332 (quant-ph)]
44. Bradshaw, M., Assad, S.M., Haw, J.Y., Tan, S.-H., Lam, P.K., Gu, M.: Overarching framework between Gaussian quantum discord and Gaussian quantum illumination. Phys. Rev. A **95**, 022333 (2017). [arXiv:1611.10020 (quant-ph)]
45. Yung, M.-H., Meng, F., Zhang, X.-M., Zhao, M.-J.: One-shot detection limits of quantum illumination with discrete signals. npj Quantum Inf. **6**, 75 (2020). [arXiv:1801.07591 (quant-ph)]